AD 700 234

# RELATIONSHIP BETWEEN FRACTURE TOUGHNESS AND ESTIMATED PLASTIC ZONE SIZE IN STEEL, TITANIUM, AND ALUMINUM ALLOYS

C. N. Freed, et al

Naval Research Laboratory
Washington, D. C.

28 November 1969

## CONTENTS

## ABSTRACT

The area of plastic deformation at a crack tip can be estimated using Irwin's plastic zone correction factor derived from linear elastic theory. The size of the plastic zone is considered to be a measure of fracture toughness, since the resistance of a metal to crack propagation is related to the deformation ahead of the crack tip.

The relationship is confirmed between fracture toughness and plastic zone size calculated from elastic considerations for steel, aluminum, and titanium alloys. Within each of the metal systems, the calculated plastic enclave increases with increasing Dynamic Tear (DT) test energy for fracture. However, the plastic zone size is an unreliable indicator of the amount of energy absorbed in the formation of the zone when a comparison is made among different metal systems. For a given size plastic enclave, the energy absorbed by the metal during the deformation process is least for aluminum alloys, while significantly greater for titanium and steel alloys in that order. When brittle alloys are compared, the difference among metal systems in the quantity of energy absorbed to form the zone is considerably diminished.

## PROBLEM STATUS

This report completes one phase of the problem; work on other aspects of the problem is continuing.

## AUTHORIZATION

NRL Problem M01-24
Project RR-007-01-46-5431

Manuscript submitted September 18, 1969.

RELATIONSHIP BETWEEN FRACTURE TOUGHNESS AND ESTIMATED PLASTIC ZONE SIZE IN STEEL, TITANIUM AND ALUMINUM ALLOYS

## INTRODUCTION

When a flaw is present in a stressed body, the stresses close to the leading edge of the crack determine its stability. As the distance from the crack tip r approaches zero, the equations describing the elastic stress field may be computed from

$$\sigma_y = K_I/\sqrt{2\pi r}\ \cos\frac{\theta}{2}\left(1 + \sin\frac{\theta}{2}\sin\frac{3\theta}{2}\right) \tag{1}$$

and

$$\sigma_x = K_I/\sqrt{2\pi r}\ \cos\frac{\theta}{2}\left(1 - \sin\frac{\theta}{2}\sin\frac{3\theta}{2}\right), \tag{2}$$

where $\sigma$ = nominal stress across the gross section and $\theta$ = polar coordinate angular measurement;

$$K = \sigma\left(W \tan\frac{\pi a}{W}\right)^{1/2}, \tag{3}$$

where a = one-half the crack length and W = specimen width. It is noted in Eq. (3) that the stress intensity parameter K incorporates specimen geometry, crack length, and applied tensile load in a single parameter (1).

Although the concentration of stresses by the flaw may produce a zone of plastic deformation at the leading edge of the crack, a small plastic enclave will not reduce the usefulness of the elastic stress field equations in describing the alteration of stresses in a body as a crack is introduced.

When $\theta = 0$, the stress field equations on the crack plane may reasonably be reduced to

$$\sigma_y \propto K_I/\sqrt{2\pi r}, \tag{4}$$

$$\sigma_x \propto K_I/\sqrt{2\pi r}, \tag{5}$$

or

$$r = (K_I/\sigma_y)\ \frac{1}{2\pi}. \tag{6}$$

In this form, the stress state in the area of stress intensification at the crack tip is described by a single stress field parameter K.

When a cracked specimen is placed in tension, the influence of the crack tip plastic zone on the elastic stress field causes the stress field to deviate from the description

given by Eqs. (1) and (2). The stress field perturbation may be approximated by including a correction to the stress value, which will account for the increase in stress in the area beyond the plastic zone caused by stress relaxation within the zone. A simpler technique is to make the approximate correction apply solely to the crack length (1). To do this, the yield stress $\sigma_{YS}$ is substituted for $\sigma_y$ in Eq. (6) to give

$$r_Y = (K_I/\sigma_{YS})^2 \frac{1}{2\pi}. \tag{7}$$

The plastic zone radius $r_Y$ approximates the distance over which stresses are relaxed due to plastic flow. The value $r_Y$ may be added to the crack length to permit the plastic zone correction to be included in the K parameter of Eq. (3). The $r_Y$ approximation has been demonstrated to be a reasonable estimate of the actual size of the plastic zone radius by Clark (2), who used an etching technique to delineate the enclave in a 3 percent silicon-iron alloy.

## $K_{Ic}$-DT CORRELATION

The Dynamic Tear (DT) test provides a sensitive and quantitative determination of the fracture toughness energy required to propagate a dynamic fracture (Fig. 1). The test is conducted under mechanical conditions of limit severity, which include a sharp, natural crack for initiation of fracture and dynamic loading. Sufficient specimen width is incorporated to develop the fracture mode characteristic of the metal. The measured energy value defines a lower limit of fracture toughness of the metal.

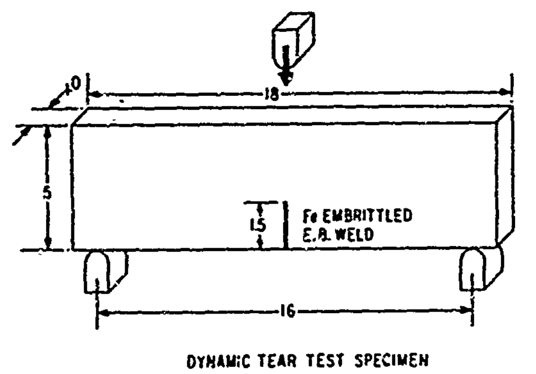


Fig. 1 - Dynamic Tear (DT) test specimen which measures the energy required to propagate a crack across the specimen width

The fracture mechanics test characterizes fracture toughness in terms of the elastic stress intensity factor $K_{Ic}$ at the point of crack instability. The $K_{Ic}$ value enables the calculation of the critical flaw size-stress level relationship as is evident from Eq. (3).

A positive correlation has been established between the $K_{Ic}$ parameter and the DT test energy values for steel, aluminum, and titanium alloys (3-5). Since plastic deformation at the crack tip is common to both the $K_{Ic}$ and DT tests, the correlation may be related to the energy absorbed by the plastic region. As the load is increased in the $K_{Ic}$ test, the elastic strain energy is balanced by the energy required for deformation at the crack tip. A load will be reached at which the elastic energy will overcome the energy needed to form the plastic enclave, and the crack will commence unstable extension. Crack propagation in the DT test also involves elastic strain energy driving the crack with resistance to propagation provided by the plastic enclave at the crack tip. Because crack movement depends on the plastic zone in both tests, the plastic zone size calculation, which involves $K_{Ic}$ values, should be related to the DT energy values. This report

describes a relationship which exists between an index of the plastic zone size and fracture toughness as measured by the DT test. A wide variety of steel, aluminum, and titanium alloys are included in the study.

## DISCUSSION

The data which were used to construct the graphs are tabulated in Tables 1 through 3 for steel, titanium, and aluminum alloys, respectively. The $K_{Ic}$ values were obtained with 1-in.-thick Single-Edge-Notched (SEN) tension specimens which were fatigued at low stress levels to form a 0.10-in. fatigue crack at the tip of the edge notch. The SEN specimen (Fig. 2) is similar in design to that employed by other NRL investigators (6), and $K_{Ic}$ was calculated using an experimental compliance calibration. Although a number of the specimens did not strictly satisfy the ASTM test procedure recommendations (7), the authors believe the values are a close approximation of $K_{Ic}$ based on findings in Refs. 8, 9, and 10.

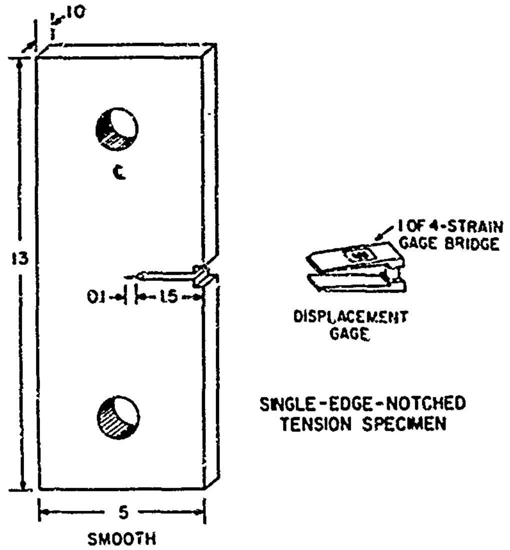


Fig. 2 - Single-Edge-Notched (SEN) tension specimen used to obtain $K_{Ic}$ values. The displacement gage is placed in the edge notch to monitor crack opening displacement.

In Fig. 3, the index of the plastic zone size is plotted against the strength-to-density ratio $YS/\rho$ for the steel, aluminum, and titanium alloys involved in this investigation. The metal systems fall into three distinct bands. For each metal an inverse relationship is evident as the plastic zone size index decreases logarithmically with an increasing $YS/\rho$. This would be expected, since the plastic zone size is a measure of toughness and fracture toughness is inversely proportional to YS.

For a given $YS/\rho$, aluminum alloys generate the smallest plastic enclave, while titanium is associated with the largest zone. Because the ordinate is a logarithmic scale, the difference among the metals is quite pronounced. For instance, at a $YS/\rho$ of 750 in., the $(K_I/YS)^2$ values are 0.078, 0.25, and 0.69 in. for aluminum, steel, and titanium, respectively. Thus, Fig. 3 indicates that for a given strength-to-density ratio, the largest plastic zone and therefore inferentially the toughest of the metals is titanium, with steel and aluminum following in that order.

Table 1
Mechanical Properties of Steel Alloys

| Material Designation | Fracture Direction | 0.2% YS (ksi) | DT Energy (ft-lb) | $K_{Ic}$ (ksi-$\sqrt{\text{in.}}$) | $(K_{Ic}/YS)^2$ (in.) | $2r_Y$ (in.) | DT/YS (ft-lb/ksi) | YS/$\rho$ ($10^3$ in.) | YS/E $\times 10^{-3}$ |
|---|---|---|---|---|---|---|---|---|---|
| J14 (9-4-0.25C) | RW | 180.0 | 1844 | 162 | 0.81 | 0.086 | 10.3 | 632 | 6.29 |
| J14 (9-4-0.25C) | WR | 180.3 | 1295 | 138 | 0.59 | 0.062 | 7.2 | 634 | 6.31 |
| J15 (9-4-0.25C) | WR | 183.2 | 2000 | 154 | 0.71 | 0.076 | 10.9 | 644 | 6.41 |
| J68 (12 Ni) | WR | 171.2* | 744 | 100 | 0.34 | 0.036 | 4.3 | 601 | 6.23 |
| J68N (12 Ni) | WR | 180.7 | 1630 | 126 | 0.49 | 0.052 | 8.7 | 644 | 6.57 |
| J70 (9-4-0.25) | WR | 176.3 | 2112 | 164 | 0.87 | 0.092 | 12.0 | 618 | 6.17 |
| J70N (9-4-0.25) | WR | 186.1 | 1280 | 153 | 0.68 | 0.072 | 6.8 | 654 | 6.50 |
| J71N (12 Ni) | WR | 174.9 | 4340 | (252) | (2.07) | (0.220) | 24.8 | 614 | 6.36 |
| J72 (12 Ni) | WR | 177.3 | 3251 | 208 | 1.38 | 0.146 | 18.4 | 622 | 6.45 |
| J72N (12 Ni) | WR | 177.1 | 3538 | 211 | 1.42 | 0.152 | 19.9 | 622 | 6.45 |
| J78 (12 Ni) | WR | 185.5 | 2271 | 155 | 0.70 | 0.074 | 12.2 | 652 | 6.75 |
| J78N (12 Ni) | WR | 189.4 | 2176 | 188 | 0.98 | 0.104 | 11.5 | 665 | 6.90 |
| J87 (9-4-0.25) | WR | 179.2 | 1996 | 163 | 0.83 | 0.088 | 11.1 | 629 | 6.26 |
| J87N (9-4-0.25) | WR | 169.7 | 2026 | 171 | 1.01 | 0.108 | 11.9 | 596 | 5.94 |
| J88 (9-4-0.25) | WR | 180.2 | 1692 | 163 | 0.82 | 0.086 | 9.4 | 632 | 6.30 |
| J88N (9-4-0.25) | WR | 168.3 | 2186 | 169 | 1.01 | 0.108 | 13.0 | 591 | 5.88 |
| H-57 (4140) | WR | 176.6 | 593 | 90 | 0.26 | 0.028 | 3.4 | 619 | 5.98 |
| D-63A (18 Ni) | RW | 229.5 | 500 | 70 | 0.09 | 0.010 | 2.1 | 805 | 8.51 |
| D-63B (18 Ni) | RW | 234.5† | 500 | 77 | 0.11 | 0.010 | 2.1 | 823 | 8.69 |

*This value is for the RW fracture direction.
†This value represents the WR fracture direction.

Table 2
Mechanical Properties of Titanium Alloys

| Material Designation | Fracture Direction | 0.2% YS (ksi) | DT Energy (ft-lb) | $K_{Ic}$ (ksi-$\sqrt{in.}$) | $(K_{Ic}/YS)^2$ (in.) | $2r_Y$ (in.) | DT/YS (ft-lb/ksi) | YS/$\rho$ ($10^3$ in.) | YS/E $\times 10^{-3}$ |
|---|---|---|---|---|---|---|---|---|---|
| T-20 Ti-6Al-4Sn-1V | RW | 127.3 | 735 | 88 | 0.45 | 0.047 | 4.25 | 777 | 7.97 |
| T-21 Ti-6Al-6V-2.5 Sn | WR | 152.0 | 275 | 61 | 0.16 | 0.017 | 1.33 | 927 | 9.51 |
| T-21A Ti-6Al-6V-2.5 Sn | RW | 166.7 | 421 | 60 | 0.13 | 0.014 | 1.86 | 1016 | 10.42 |
| T-21B Ti-6Al-6V-2.5 Sn | RW | 129.7 | 550 | 82 | 0.40 | 0.042 | 3.11 | 792 | 8.12 |
| T-21B Ti-6Al-6V-2.5 Sn | WR | 135.6 | 743 | 78 | 0.33 | 0.035 | 4.02 | 827 | 8.48 |
| T-21C Ti-6Al-6V-2.5 Sn | RW | 137.2 | 500 | 81 | 0.35 | 0.037 | 2.68 | 837 | 8.58 |
| T-21C Ti-6Al-6V-2.5 Sn | WR | 137.2 | 717 | 74 | 0.29 | 0.031 | 3.84 | 837 | 8.58 |
| T-21D Ti-6Al-6V-2.5 Sn | RW | 186.0 | 185 | 34 | 0.03 | 0.003 | 0.73 | 1158 | 11.61 |
| T-23 Ti-8Al-2Cb-1Ta | RW | 112.0 | 1750* | 118 | 1.11 | 0.118 | 11.50 | 683 | 7.00 |
| T-27A Ti-6Al-4V | RW | 132.5 | 1251 | 112 | 0.72 | 0.076 | 6.96 | 808 | 8.30 |
| T-27A Ti-6Al-4V | WR | 140.1 | 930 | 108 | 0.60 | 0.064 | 4.88 | 860 | 8.76 |
| T-36 Ti-6.5Al-5Zr-1V | WR | 124.5 | 960 | 97 | 0.61 | 0.065 | 5.67 | 760 | 7.79 |
| T-55A Ti-6Al-4Zr-2Mo | WR | 135.7 | 990 | 115 | 0.72 | 0.076 | 5.37 | 827 | 8.28 |
| T-55B Ti-6Al-4Zr-2Mo | WR | 132.0 | 748 | 99 | 0.56 | 0.059 | 4.17 | 805 | 8.25 |
| T-67 Ti-6Al-4V-2 Sn | RW | 115.8 | 886 | 104 | 0.81 | 0.086 | 5.65 | 705 | 7.34 |
| T-67A Ti-6Al-4V-2 Sn | RW | 129.8 | 540 | 83 | 0.41 | 0.044 | 3.06 | 792 | 8.12 |
| T-67B Ti-6Al-4V-2 Sn | RW | 122.0 | 900 | 104 | 0.73 | 0.077 | 5.42 | 745 | 7.64 |
| T-68A Ti-6Al-4Zr-2 Sn-0.5 Mo-0.5V | RW | 117.5 | 1385 | 124 | 1.11 | 0.117 | 8.68 | 717 | 7.35 |
| T-68B Ti-6Al-4Zr-2 Sn-0.5 Mo-0.5V | RW | 119.2 | 1470 | 115 | 0.93 | 0.099 | 9.07 | 728 | 7.46 |
| T-68D Ti-6Al-4Zr-2 Sn-0.5 Mo-0.5V | RW | 121.3 | 1043 | 131 | 1.17 | 0.124 | 6.34 | 741 | 7.59 |
| T-68E Ti-6Al-4Zr-2 Sn-0.5 Mo-0.5V | RW | 121.5 | 1182 | 127 | 1.09 | 0.116 | 7.18 | 742 | 7.60 |

*This DT test value represents the WR fracture direction.

Table 3
Mechanical Properties of Aluminum Alloys

| Material Designation | Fracture Direction | 0.2% YS (ksi) | DT Energy (ft-lb) | $K_{Ic}$ (ksi-$\sqrt{in.}$) | $(K_{Ic}/YS)^2$ (in.) | $2r_Y$ (in.) | DT/YS (ft-lb/ksi) | YS/ρ ($10^3$ in.) | YS/E $\times 10^{-3}$ |
|---|---|---|---|---|---|---|---|---|---|
| 2020-T651 | WR | 76.3 | 78 | 16.5 | 0.047 | 0.005 | 1.03 | 703 | 6.80 |
| 2024-T4 | RW | 48.1 | 490 | 47.4 | 0.971 | 0.103 | 10.10 | 401 | 4.54 |
| 2024-T351 | WR | 43.9 | 206 | 31.0 | 0.500 | 0.053 | 4.70 | 430 | 4.14 |
| 2219-T87 | RW | 57.9 | 207 | 33.3 | 0.332 | 0.035 | 3.57 | 570 | 5.57 |
| 2219-T87 | WR | 55.2 | 207 | 30.1 | 0.298 | 0.032 | 3.75 | 552 | 5.30 |
| 2219-T851 | RW | 56.5 | 360 | 36.0 | 0.392 | 0.041 | 6.40 | 503 | 5.70 |
| 2219-T851 | WR | 58.4 | 208 | 38.0 | 0.424 | 0.045 | 3.50 | 564 | 5.61 |
| 7075-T6 | RW | 78.5 | 110 | 33.1 | 0.178 | 0.019 | 1.40 | 795 | 7.55 |
| 7075-T6 | WR | 77.0 | 102 | 24.0 | 0.098 | 0.020 | 1.31 | 778 | 7.40 |
| 7075-T7351 | RW | 66.7 | 249 | 33.3 | 0.249 | 0.026 | 3.74 | 667 | 6.41 |
| 7075-T7351 | WR | 64.9 | 146 | 27.0 | 0.173 | 0.018 | 2.27 | 649 | 6.24 |
| 7079-T6 | WR | 74.0 | 83 | 21.7 | 0.084 | 0.009 | 1.09 | 749 | 7.20 |
| 7106-T63 | WR | 62.5 | 424 | 41.7 | 0.030 | 0.007 | 6.00 | 626 | 6.00 |

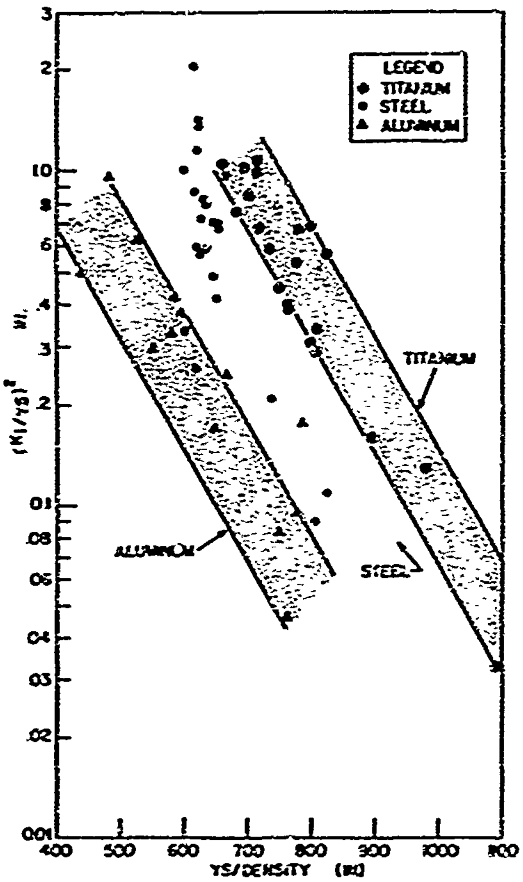


Fig. 3 - Comparison of the yield strength-to-density ratio to an index of the plastic zone size $(K_I/YS)^2$

A similar conclusion may be drawn from Fig. 4 in which the plastic zone index is compared with YS normalized by the Modulus of Elasticity E. An inverse relationship is manifested between $(K_I/YS)^2$ and the yield strength-to-modulus ratio, and the relative ordering of the metal systems in terms of increasing toughness is aluminum, steel, and titanium. The increased scatter of data points at high $(K_I/YS)^2$ values, for steel alloys in Figs. 3 and 4, may be a reflection of the decreasing accuracy of $K_{Ic}$ values for alloys exhibiting considerable fracture toughness.

The inferences drawn from Figs. 3 and 4 are disputed by the results depicted in Fig. 5. When the plastic zone size index is plotted against DT energy, the order of toughness between steel and titanium alloys is reversed. For any $(K_I/YS)^2$ value above 0.1 in., it is evident that steel alloys are associated with far higher DT energy values than the titanium alloys. Thus, for a given plastic zone size, the energy required to create the plastically deformed enclave cannot be accurately discerned by a normalized YS criteria, such as was employed in Figs. 3 and 4.

Within a metal system, the size of the plastic zone may be an adequate standard to estimate the relative toughness of different alloys. In Fig. 5 the plastic zone size index increases as the DT energy is increased for each of the three metal systems indicating that the enclave size is related to the deformation energy required to produce the enclave.

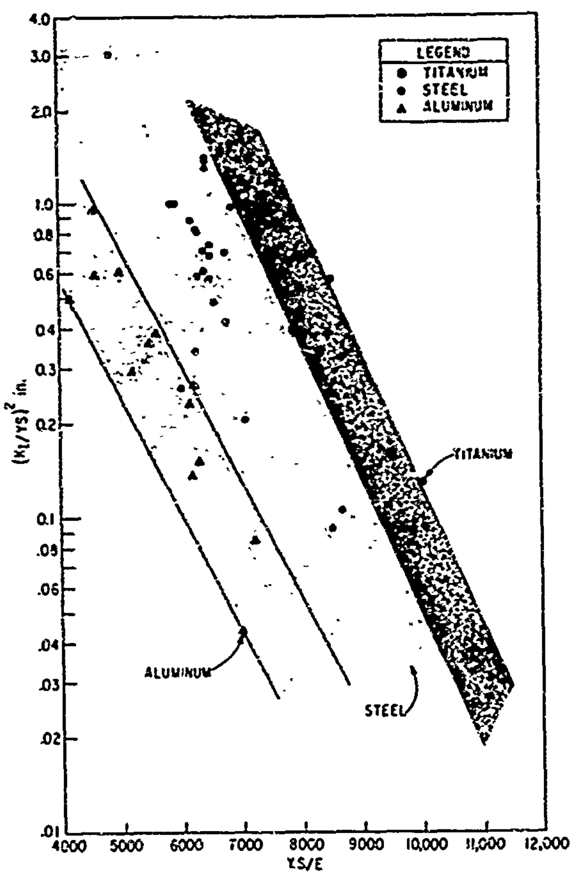


Fig. 4 - The yield strength-to-modulus ratio vs the plastic zone size index for a variety of steel, titanium, and aluminum alloys

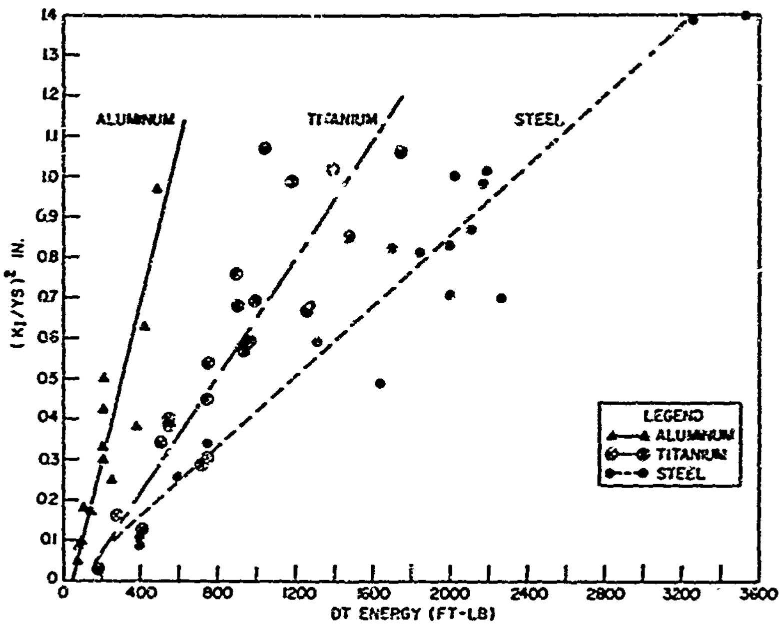


Fig. 5 - Relationship of the plastic zone size index to the energy required to create the zone. The DT energy value indicates the resistance of the metal to crack propagation due to the plastic deformation at the crack tip.

However, plastic zone size is not a reliable indicator of the amount of energy absorbed in creating the zone when different metal systems are compared. As Fig. 5 indicates when the energy to form the zone is plotted on the abscissa in place of a normalized YS factor, the order of toughness of the metals may be affected, although for very brittle alloys which are associated with small plastic zones, it is more difficult to discern the influence of the metal system on the energy required to cause plastic deformation. From the viewpoint of rating metal systems as to their resistance to crack propagation, the criterion of enclave size may be misleading if other mechanical and metallurgical aspects of the deformation process are not also considered.

The fracture toughness-yield strength relationship for steel, titanium, and aluminum alloys is plotted in Fig. 6. The curve for each of these metals is the Technological Limit Line which represents the toughest alloys produced for a given YS as defined by all data available to date. The correlation between $K_{Ic}$ and DT energy for these metals enables the estimation of $K_{Ic}$ values from DT energy values and the subsequent conversion of the $K_{Ic}$ number into a flaw size-stress level relationship.

Each of the Technological Limit curves has been overlaid with two lines: the solid line is defined as the $K_{Ic}$/YS upperbound for 1-in.-thick specimens using ASTM criteria, and the dashed line indicates an approximate $K_Q$/YS upper boundary. Those alloys which have $K_{Ic}$/YS ratios below the ASTM line represent alloys from which $K_{Ic}$ values can be obtained which are in accord with ASTM standards for 1-in. plate (7). The $K_Q$/YS ratio line indicates a tougher region in which investigators have found the $K_Q$ values equal to or approximately $K_{Ic}$ (8-10).

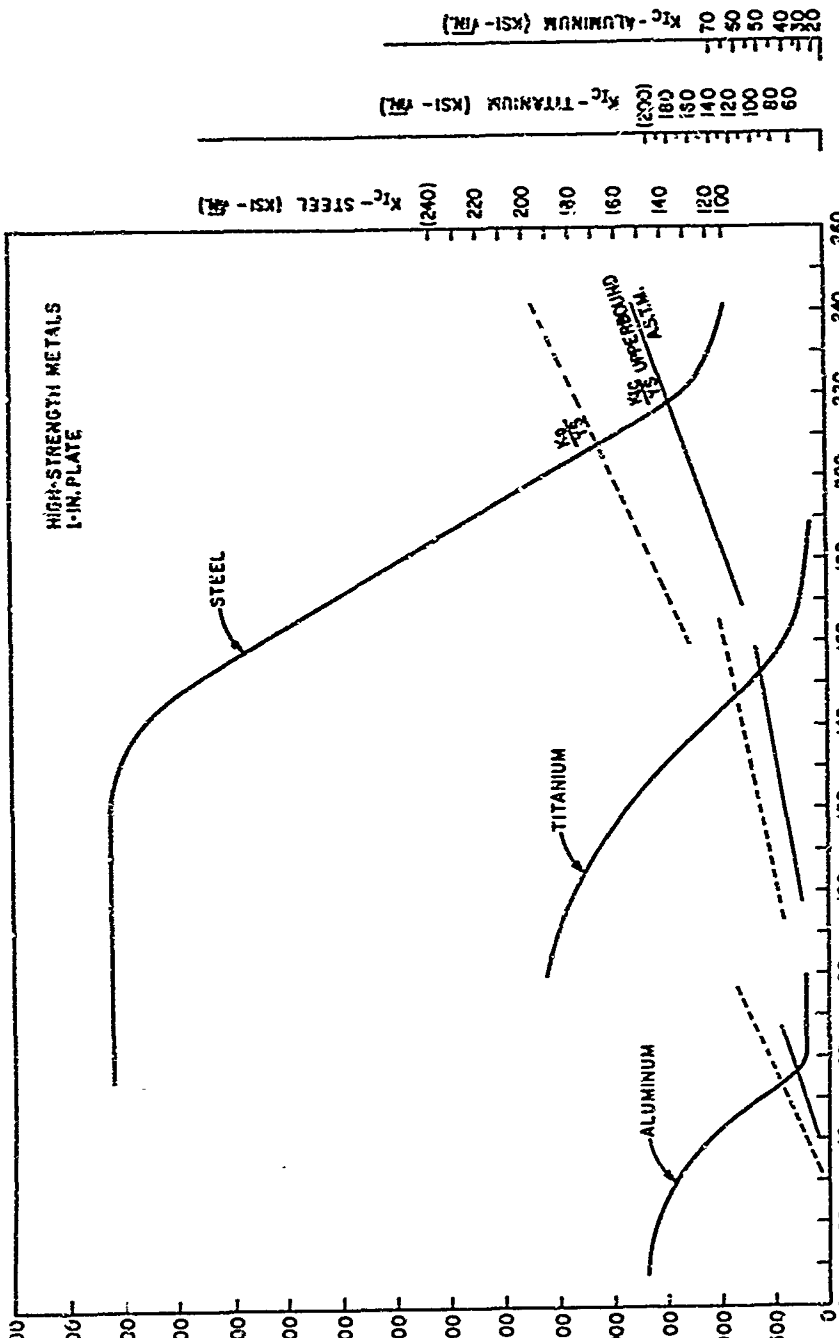


Fig. 6 - A comparison of the Technological Limit Lines for steel, aluminum, and titanium alloys. The $K_{Ic}$/YS lines indicate the ASTM limits for $K_{Ic}$ values obtained with 1-in.-thick plate.

The area below the $K_Q$/YS ratio lines on the Technological Limit (T.L.) curves in Fig. 6 demonstrates the restricted toughness range over which plane strain fracture mechanics is applicable relative to the full toughness spectrum for each metal system. Further, the absolute toughness difference between the upperbound ASTM plane strain line and the upper shelf of these strength transition curves varies markedly among the metal systems. While 250 ft-lb correspond to the ASTM upperbound ratio value for 1-in.-thick aluminum alloys on the T.L. curve, the toughest aluminum alloys represented by the upper shelf require only about 1700 ft-lb of energy to propagate a crack in a DT specimen. When this 1450-ft-lb difference is compared to a 5000-ft-lb difference found for steel alloys, it becomes evident that not only do the toughest aluminum alloys require considerably less energy to move a crack than either steel or the intermediate titanium alloys, but the toughness range over which the other metals will fail by stable crack propagation is much larger than for aluminum alloys.

It should be noted that when the $K_{Ic}$/YS ratio of the metal approaches the ASTM upperbound value there is no assurance that initial elongation of a pre-existing crack will result in continued unstable crack propagation, although the ratio meets ASTM standards. Some crack growth may be required before the critical crack length-stress level relationship is attained which is sufficient to cause unstable propagation. To the designer-engineer, the ability to predict the onset of initial crack movement which is followed by either stable growth or crack arrest is of limited usefulness. The development of a test procedure which will allow determination of the stress-flaw size relationship for a stress state other than plane strain is needed to analyze the alloys which lie above the $K_{Ic}$/YS upperbound but which are still subject to crack propagation under elastic loading conditions. This procedure would also aid the designer in the interpretation of $K_{Ic}$ values which are characterized by stable crack growth following initial crack movement.

The approximation of the plane strain plastic zone size $2r_Y$ is compared to the DT energy normalized by YS for steel, titanium, and aluminum alloys in Figs. 7, 8, and 9, respectively. The normalization of the DT energy has the effect of reducing the scatter present in Fig. 5. These graphs permit the estimation of the size of the plastically deformed enclave from the mechanical properties derived from two straightforward engineering tests.

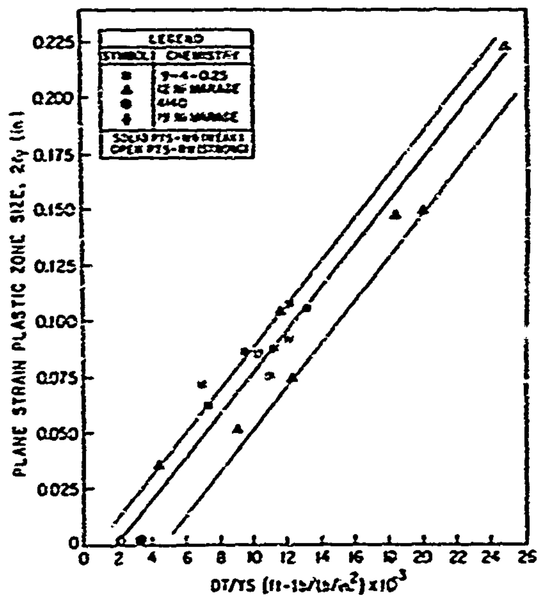


Fig. 7 - Comparison of DT energy normalized by YS to the plane strain plastic zone size ($2r_Y$) for steel alloys

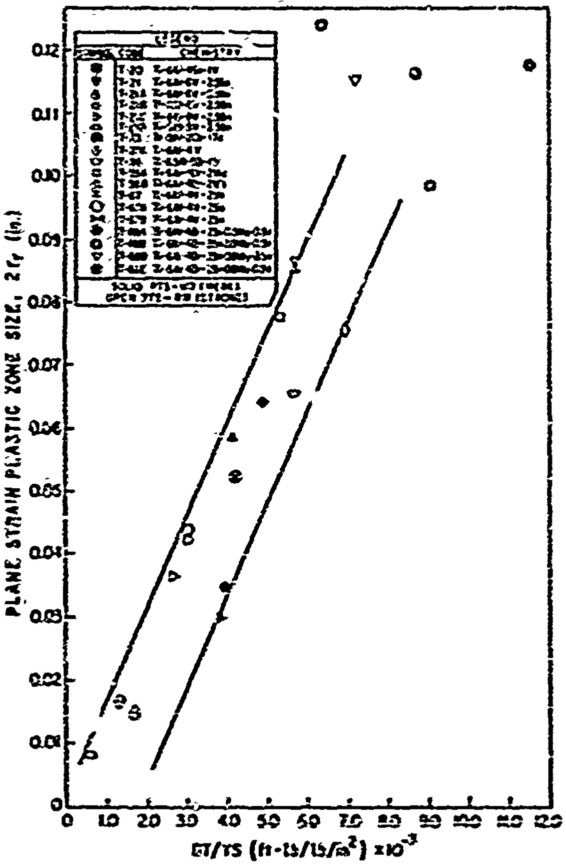


Fig. 8 – Comparison of DT energy normalized by YS to the plane strain plastic zone size for titanium alloys

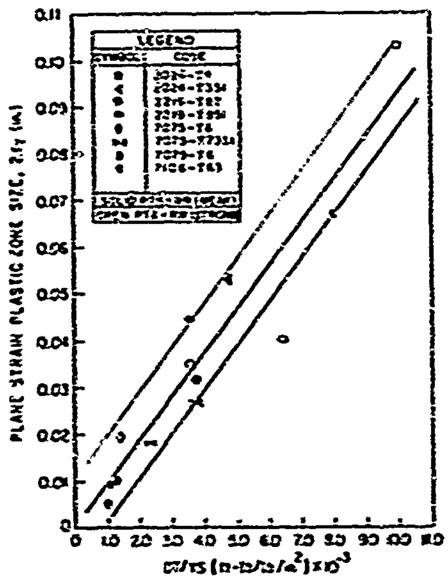


Fig. 9 – Comparison of DT energy normalized by YS to the plane strain plastic zone size for aluminum alloys

## CONCLUSIONS

1. The size of the plastic zone as determined by Irwin's correction formula is an adequate representation of the fracture toughness for steel, titanium, or aluminum alloys. Within each of these metal systems, the plastic enclave size increases as the DT energy required for crack propagation is increased.

2. The plastic zone size is not a reliable indicator of the amount of energy absorbed in creating the zone when a comparison is made among metal systems. Even though the same plastic zone size is indicated by an aluminum, a titanium, and a steel alloy, the energy absorbed by plastic flow within the enclave will be considerably different for each metal except for the most brittle alloys.

## REFERENCES


1. "Fracture Testing of High-Strength Sheet Materials: A Report of a Special ASTM Committee," ASTM Bull. 243:29-40 (1960)

2. Clark, W.G., Jr., "Visual Observation of the Crack Tip Plastic Zone Developed in a 3 percent Si-Fe Alloy," Westinghouse Research Laboratories Scientific Paper 66-1D6-BTLFR-P1, Sept. 27, 1966

3. Freed, C.N., and Goode, R.J., "Correlation of Two Fracture Toughness Tests for Titanium and Ferrous Alloys," NRL Report 6740, Jan. 16, 1969

4. Freed, C.N., "A Comparison of Fracture Toughness Parameters for Titanium Alloys," Eng. Fracture Mech. 1 (No. 1):175-189 (1968)

5. Freed, C.N., Goode, R.J., and Judy, R.W., Jr., "Comparison of Fracture Toughness Test Procedures for Aluminum Alloys," NRL Report 6853, Feb. 17, 1969

6. Sullivan, A.M., "New Specimen Design for Plane-Strain Fracture Toughness Tests," Mater. Res. Std. 4 (No. 1):20-25 (1964)

7. ASTM Standards 31:1099 (1969)

8. Freed, C.N., and Krafft, J.M., "Effect of Side Grooving on Measurements of Plane-Strain Fracture Toughness," J. Mater. 1 (No. 4):770-790 (1966)

9. Wessel, E.T., "State of the Art of the WOL Specimen for $K_{Ic}$ Fracture Toughness Testing," Eng. Fracture Mech. 1 (No. 1):77-103 (1968)

10. Barsom, J.M., and Rolfe, S.T., "$K_{Ic}$ Transition Temperature Behavior of A-517-F Steel," U.S.S. Applied Research Laboratory Report 89.018-022(1), Nov. 29, 1968

Security Classification

**DOCUMENT CONTROL DATA - R & D**

(Security classification of title, body of abstract and indexing annotation must be entered when the overall report is classified)

| | |
|---|---|
| 1. ORIGINATING ACTIVITY (Corporate author) <br> Naval Research Laboratory <br> Washington, D.C. 20390 | 2a. REPORT SECURITY CLASSIFICATION <br> Unclassified <br> 2b. GROUP |

3. REPORT TITLE

RELATIONSHIP BETWEEN FRACTURE TOUGHNESS AND ESTIMATED PLASTIC ZONE SIZE IN STEEL, TITANIUM, AND ALUMINUM ALLOYS

4. DESCRIPTIVE NOTES (Type of report and inclusive dates)

Final report on one phase of the problem; work is continuing on other phases.

5. AUTHOR(S) (First name, middle initial, last name)

C.N. Freed and R.J. Goode

| 6. REPORT DATE | 7a. TOTAL NO. OF PAGES | 7b. NO. OF REFS |
|---|---|---|
| November 28, 1969 | 18 | 10 |

| | |
|---|---|
| 8a. CONTRACT OR GRANT NO. <br> NRL Problem M01-24 <br> b. PROJECT NO. <br> RR-007-01-46-5431 <br> c. <br> d. | 9a. ORIGINATOR'S REPORT NUMBER(S) <br> NRL Report 6991 <br> 9b. OTHER REPORT NO(S) (Any other numbers that may be assigned this report) |

10. DISTRIBUTION STATEMENT

This document has been approved for public release and sale; its distribution is unlimited.

| | |
|---|---|
| 11. SUPPLEMENTARY NOTES | 12. SPONSORING MILITARY ACTIVITY <br> Department of the Navy <br> (Office of Naval Research), <br> Washington, D.C. 20360 |

13. ABSTRACT

The area of plastic deformation at a crack tip can be estimated using Irwin's plastic zone correction factor derived from linear elastic theory. The size of the plastic zone is considered to be a measure of fracture toughness, since the resistance of a metal to crack propagation is related to the deformation ahead of the crack tip.

The relationship is confirmed between fracture toughness and plastic zone size calculated from elastic considerations for steel, aluminum, and titanium alloys. Within each of the metal systems, the calculated plastic enclave increases with increasing Dynamic Tear (DT) test energy for fracture. However, the plastic zone size is an unreliable indicator of the amount of energy absorbed in the formation of the zone when a comparison is made among different metal systems. For a given size plastic enclave, the energy absorbed by the metal during the deformation process is least for aluminum alloys, while significantly greater for titanium and steel alloys in that order. When brittle alloys are compared, the difference among metal systems in the quantity of energy absorbed to form the zone is considerably diminished.

DD FORM 1 NOV 65 1473 (PAGE 1)

S/N 0101-807-6801



Security Classification

| 14 KEY WORDS | LINK A | | LINK B | | LINK C | |
|---|---|---|---|---|---|---|
| | ROLE | WT | ROLE | WT | ROLE | WT |
| Steel alloys | | | | | | |
| Aluminum alloys | | | | | | |
| Titanium alloys | | | | | | |
| Fracture toughness | | | | | | |
| Plastic zone size | | | | | | |
| Plastic zone energy | | | | | | |
| Dynamic Tear Test | | | | | | |